EXPERIMENTAL STUDY ON THE SHEAR ADHESION STRENGTH BETWEEN THE ICE AND SUBSTRATE IN ICING WIND TUNNEL

C. X. Zhu C. L. Zhu* W. W. Zhao M. J. Tao

Key Laboratory of Fundamental Science for National Defense-Advanced Design Technology of Flight Vehicle
Nanjing University of Aeronautics and Astronautics
Nanjing, China

ABSTRACT

The icing wind tunnel can simulate the air flow at a high altitude; such an air flow contains supercooled droplets moving at certain velocities. An integrated experiment method was proposed, and it included the icing test and shear stress measurements in the simulated environment of the icing wind tunnel. The error caused by the change in experimental environments was completely eliminated with this novel method. Thus, there was no discrepancy between the real-time and experimental values of shear stress between the ice and substrate. The experiments of icing and shear stress measurements are carried out by varying the following parameters: icing temperature, mean volume diameter (MVD) of droplets, and surface roughness of the substrate. The results indicate that the shear stress between the ice and the substrate increases with the decrease in temperature provided the temperature is relatively high. When the MVD value is 22 μm, the liquid water content is about 1 g/m^3 and surface roughness is 2 μm. Under these conditions, the shear stress reaches its maximum value at a temperature of –15°C. The shear stress is also affected by the MVD values of droplets, and the surface roughness of substrate.

Keywords: Shear stress, Icing wind tunnel, Integrated experiment method, Meteorological parameters.

1. INTRODUCTION

Icing will occur on the windward surface when the aircraft flies through the clouds, which contain super cooled droplets. Icing alters the aerodynamic shape of the aircraft. Consequently, the aerodynamic performance of the aircraft deteriorates, and the maneuverability and stability of the aircraft also diminishes during flight. To ensure flight safety, aircraft engineers need to develop and install ice protection systems immediately. Because of its several advantages, the mechanical de-icing system is one of the most important components of aircraft icing protection systems: some of its advantages include a simple structure, high reliability, and low power consumption. However, a complicated process is involved when de-icing is carried out with the aforementioned mechanical system [1]. In this process, operators can remove ice from the aircraft's surface only when they are able to destroy the shear stress or the normal stress of the interface between ice and aircraft skin. In previous research studies, it has been established that between ice and aircraft skin, the shear stress is much smaller than the normal stress. Thus, these studies imply that the shear stress can be overcome easily by applying an external force of lower magnitude. Following the successful suppression of shear stress, aircraft maintenance operators can easily detach the ice from the surface even under the effect of aerodynamic forces. With this approach, de-icing can be achieved completely. In recent years, quite a few research studies have focused their attention on developing an ultrasonic de-icing system that is based on the principle of de-icing. To design and develop a novel de-icing device, such as the ultrasonic de-icing system, scientists need to comprehensively understand the intrinsic material properties and the adhesion strength of impact ices [2-3].

In the current studies of icing mechanics, scientists mainly describe the following three aspects: i) the ice adhesion mechanism; ii) the measurement of adhesion strength of ice; and iii) the determination of mechanical properties of ice, including tensile strength and shear strength. Fortin described adhesion mechanism with the molecular mechanism [4]. Petrenko's study illustrated that hydrogen bond maybe was the most important factor in the mechanism of adhesion [5]. Using two sets of cylindrical tubes, Chu determined shear stress, roughness, and median volume diameters (MVDs) under different ice temperatures [1,6]. In 1980s, Druez per-

* Corresponding author (clzhu@nuaa.edu.cn)

DOI : 10.1017/jmech.2017.83
Copyright © 2017 The Society of Theoretical and Applied Mechanics
https://doi.org/10.1017/jmech.2017.83 Published online by Cambridge University Press

formed tensile testing using aluminum tube [7]. Jellinek measured the tensile strength and adhesion strength of ice by introducing pure water between two metallic cylinders [8]. Stallabrass and Price studied the adhesion strength of ice on different surfaces, and they found that the adhesion effect was the same provided the base material was prepared from polytetrafluoroethylene (PTFE) and any metal [9,10]. Miller and Bond determined the adhesion effect in rotating blades, and the test results prove that icing leads to an increase in blade torque. In addition, the vibration of the blade detaches the ice, which is an undesirable effect [11]. To determine the tensile strength and elastic modulus of ice specimens, Reich performed bending test on ice specimens using backing foil in the first instance and then repeated the test without using backing foil [12]. Li Hongsheng investigated the constitutive equation of ice performance and established a prediction model of the ductile-brittle transition point [13]. Yue Qianjin designed a new experimental device for sea ice [14]. Liu Weibo determined the torsional strength and shear elastic modulus of ice at certain temperatures to estimate different rates of shear strain. For this purpose, Liu performed torsion experiments using freshwater ice [15]. Anderson conducted experiments to explore the strength of ice adhesion in the IRT [16]. The ice was frozen between the fixed plate and movable deck through which a length of pipe filled with circulating alcohol passes to decrease the temperature. During the experiment, the ice adhesion strength was evaluated by the measurement of load used to move the deck. The strength of the adhesion of ice on a variety of materials was successfully measured experimentally. But the subsequent research shows that there are some loopholes in this method, and a gap was found between the experimental results and the followings. Ivan and Victor studied the mechanism of ice adhesion theoretically [17]. They believe that besides the Van der Waals force and the chemical bonding mechanism, electrostatic interaction also contributes greatly to the adhesion of ice. For this, they investigated a simple theoretical model basing on the theory of ice surface electrical properties. The results show that the electrostatic model gives the correct order of magnitude of ice adhesion, and the energy provided by electrostatic interaction is obviously higher than that of the other two, and plays an important role in ice adhesion. The success of the study provides an intuitive way to understand time and temperature dependent phenomena which helps to explain differences in ice properties. Their research provides some guidance to the following experiments. Yin [18], Wang [19] and Haneesh [20] had studied the effects of surface microstructure, temperature and surface roughness on the ice adhesion strength. It can be seen that all these factors have effects on the ice adhesion strength. But the experimental results also indicate that shear stress of ice and its substrate have not been studied systematically until now. In most experiments, icing test is carried out first. Then, the specimens covered with ice are taken out from the icing environment and placed in another environment for the purpose of determining shear force. Thus, there may be some discrepancies between the experimental and the real values of shear force.

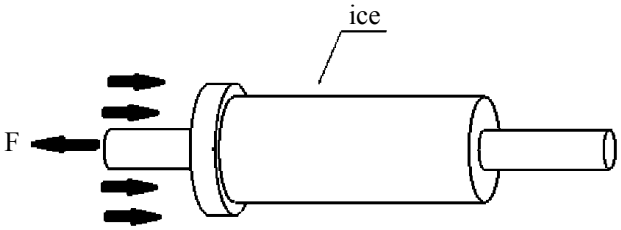


Fig. 1 The graph of principle of shear stress measure.

In this study, an integrated experimental method was developed to include both the icing test and shear stress measurements; this method is based on the icing wind tunnel that simulates the air flow field with super-cooled droplets in flights. While performing the experimental test, we are able to control the temperature and MVD accurately. Using this experimental method, we determined the characteristics of shear stress in ice and its substrate under the following different conditions: various ice temperatures, various substrate surface roughness, and various MVDs of droplets. The effects of these parameters on the shear stress are obtained with the novel method, and the experimental results serve as the basis for developing the design of the mechanical de-icing system.

2. EXPERIMENTAL METHODS

2.1 Shear Stress Measurement Principle

Figure 1 illustrates the principle on which the measurement of shear stress is based in this experiment. Because ice accumulates in the center of the cylindrical surface, an external force is applied at the extreme left end of the ice layer. Then, there will be relative displacement between the ice and the substrate; however, the magnitude of this displacement is very small. The relative displacement occurs when the ice detaches from the substrate. At this stage, the applied force reaches its maximum value, so the magnitude of the force is the value of the shear force at the interface. Based on this principle, we developed an integrated experimental method for icing. As shown in Fig. 2, the shear force is measured in an icing wind tunnel. The test specimen is connected with the sensor through the coupler and its end is inserted into the sleeve. In the experimental section, the test specimen is placed at the center of the icing wind tunnel, and it is supported by the strut. To ensure coaxiality, we adjust the relative position of the open pore of the sleeve and the test specimen before performing the experiment.

In this experimental study, the size of all the test specimens was the same regardless of the cases being analyzed in the apparatus. The diameter of the cylindrical specimen is 1 cm, and the length of the specimen is 20 cm. The distance between the axis of the cylin-

https://doi.org/10.1017/jmech.2017.83 Published online by Cambridge University Press

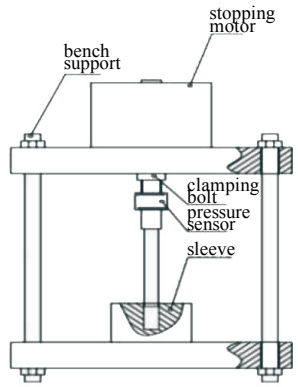


Fig. 2 A schematic diagram of shear force measurements.

Table 1 Stepping motor performance parameters.

Parameters	Value
Step angle/°	1.8
Fuselage length/mm	56
current/A	2
resistance/Ω	1.8
inductance/mH	2.5
Static moment/kg·cm Min	9.0
Positioning moment/N·cm Max	3.5
Moment of inertia/g·cm^2	280
Lead number	5

drical specimen and the wall of icing wind tunnel is about 20 cm. Because the test specimen is installed vertically, therefore, the test results are not affected by blocking effects.

The motor that drives the rotation of the test specimen is inclined at a step angle of 1.8 degrees, and it is excited by a sinusoidal signal. The relationship between the speed and frequency of the motor is shown as follows:

$$m = \frac{50000}{60} n \tag{1}$$

Where m is the signal frequency (Hz), and n is the motor speed (rad/min). In order to cooperate with the acquisition module, the motor is rotated under the excitation of a sinusoidal wave signal of 5000 Hz. The resultant data is recorded per second. The specific parameters of the motor are shown in Table 1.

A piezoresistive sensor is used in the motor, and the changes in pressure are induced by four electric resistance strain elements. The input voltage of the sensor is maintained at 10 V throughout the experiment. Moreover, the output voltage is varied from 0 to 20 MV; the output voltage characteristic is linear with the measured force. The main performance parameters of the sensor are presented in Table 2.

During the experiment, the ADMA acquisition module

Table 2 Performance parameters of the sensor.

parameters	Value
accuracy	0.05%
sensitivity	2mV/V
creep	±0.05%/30 min
Nonlinear	±0.05%
Lag error	±0.03%
Repetitive error	±0.03%
zero temperature	±0.03%/10°C
Output temperature coefficient	±0.03%/10°C
Operating temperature range	-20~70°C
Bridge voltage	5~15VDC

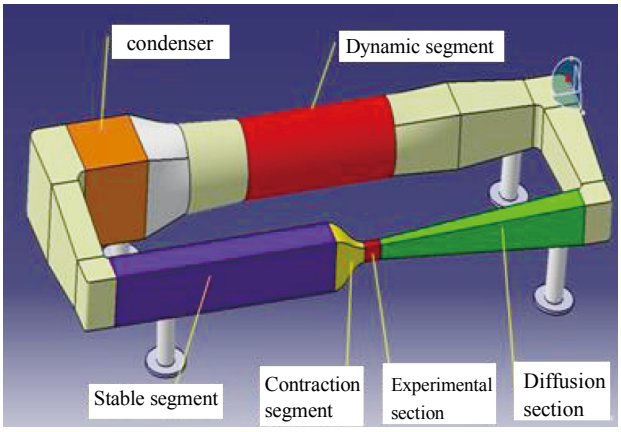


Fig. 3 A Schematic diagram of icing wind tunnel.

was used to transfer the output voltage of the sensor into the computer. The AD conversion accuracy of the ADMA acquisition module is 16 bits; the resolution is up to 1 μV, and the acquisition precision is about 0.00001.

2.2 Icing Wind Tunnel

Figure 3 provides a schematic representation of icing wind tunnel: it is mainly composed of air duct, refrigeration system, and spray system. The main components of the icing wind tunnel are as follows: test section, diffuser, corner, power plant, heat exchanger section, settling chamber, and contraction. There are two frequency conversion motors functioning at 110 kW power; these motors regulate the air velocity of the duct. The second and third corners are equipped with a water-circulating heating system, which prevents local icing. The size of test section is 0.5 m × 0.3 m × 0.4 m. The continuous working time of the tunnel is 4 hours. The spray system is installed into the settling chamber. Furthermore, the specific parameters of other devices are presented in Table 3.

2.3 Test Procedure

To determine the shear adhesion strength of ice at the

https://doi.org/10.1017/jmech.2017.83 Published online by Cambridge University Press

Table 3 Parameters of icing wind tunnel.

parameters	value
size	500 mm × 300 mm × 400 mm
wind speed	0 m/s – 100 m/s
temperature	Range: room temperature～–45°C Cooling speed: from 20 to –20 degrees Celsius, 25 min Uniformity: ≤1°C error: ±0.5°C
humidity Cloud parameters	Range: 70 – 100% (–15°C – –20°C); 100% (–20°C – –45°C) Error: ±5% LWC: 0.1 g/m^3 – 3 g/m^3 MVD: 10 – 300 μm Uniformity: Experimental range 60%

interface of ice layers and substrates, we performed the following conventional testing methods: icing tests and the shear adhesion strength measurement. Both the testing methods were carried out in a standard icing wind tunnel under the same icing meteorological conditions. With this modified strategy, we eliminated the errors introduced by conducting the analyses of test specimens in different environments. Thus, the discrepancy in the experimental and real values of shear adhesion strength was minimized effectively. The main steps of the test procedure are as follows:

(1) Run the wind tunnel, and turn on the refrigeration compressor to lower the temperature.

(2) Open the motor, and make sure that the test piece rotates evenly. The wind tunnel continues to cool the flow field. When the temperature reaches the test value, test piece should stop rotating. At this point of time, measure the shear force without loads; shear force measurements must be repeated in triplicates to confirm the reproducibility of results.

(3) Turn on the spray system, and regulate the pressure of water and air in order to obtain an exact MVD.

(4) To maintain the aforementioned test conditions, lock the bolt tightly and precess the screw. Then, start the collecting module to record simultaneously the data of shear adhesion strength of various ice layers.

(5) Switch off the refrigeration compressor when the recording ends, and start sweeping the tunnel to get prepared for the next test.

3. EXPERIMENTAL RESULTS AND ANALYSIS

Dozens of tests are carried out in various conditions by implementing the proposed method described in this paper. Figure 4 illustrates the experimental set up used to conduct icing test and shear stress test in an icing wind tunnel. The freezing temperature varies from –4 to –18°C. The parameter MVD varies from 20 to 40 μm. The surface roughness of the substrate material varies from 3 to 33 μm. In all the cases, the liquid water content is about 1.0 g/m^3.

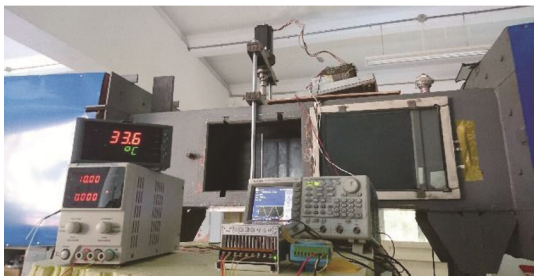


Fig. 4 Picture of icing test and shear stress test in icing wind tunnel.



Fig. 5 Ice photo on the test model at temperature of -5°C.

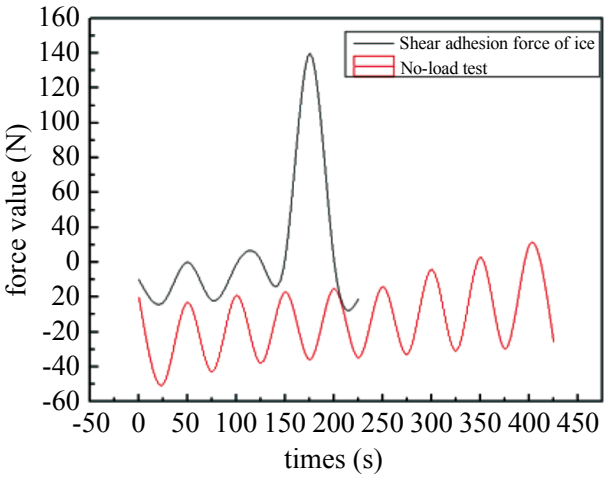


Fig. 6 Curve of force.

3.1 Effects of Freezing Temperature

Except for temperature, the remaining experimental parameters are kept constant. The main parameters in the experiment are as follows: the loading speed is 0.00375 cm/s; the surface roughness of the aluminum rod is 3.19 μm; the freezing time is 4 minutes, and MVD is 22 μm.

Now, the experiment was performed at a temperature of –5°C. Figure 5 displays ice accretion on the cylindrical specimen. Figure 6 is a plot illustrating the re-

https://doi.org/10.1017/jmech.2017.83 Published online by Cambridge University Press

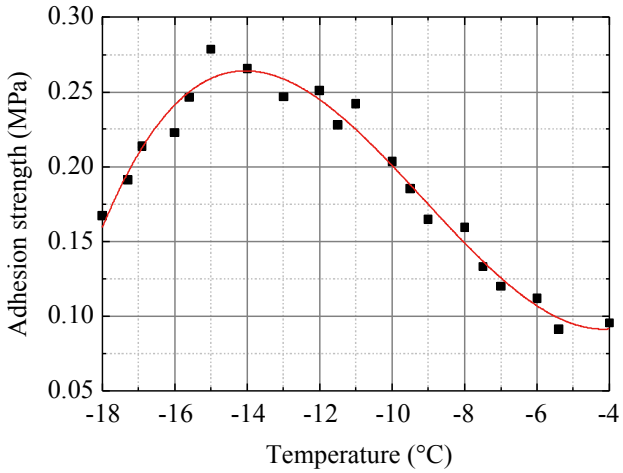


Fig. 7 Shear adhesion strength of impact ice at different temperatures.

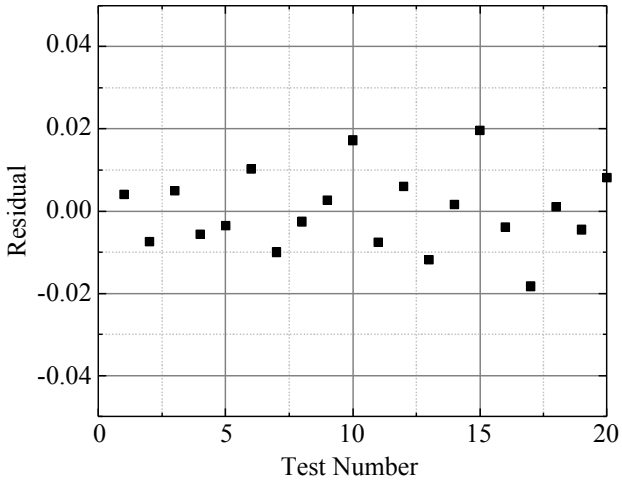


Fig. 8 The difference between the experimental data with the calculation results using the formula.

sults of shear adhesion strength obtained by the shear stress measurement test. The black curve illustrates the relationship between the external loading and time period during which the test specimen was covered with ice, while the red curve illustrates the relationship between the external loading and time period during which the test specimen was clean. With the passage of time, the external force increases steadily until it reaches its maximum value. At this stage, the adhesion between the ice and its substrate ceases completely. At this stage, the difference between the loading values in the black and red curves is the magnitude of the shearing force at the interface. The following formula is used to calculate the shear adhesion strength of ice in the experiment.

$$A_d = \frac{F_t}{s} \tag{2}$$

Where A_d is the shear adhesion strength of ice (Pa); F_t is the shear adhesion force (N), and s refers to the contact area between the ice layer and the substrate (m^2).

By adopting the proposed method of measurement and data processing, we obtained the experimental results of the shear force between the ice and substrate.

As shown in Fig. 7, the horizontal axis represents temperature (°C), whereas the vertical axis represents the shear adhesion strength (MPa) corresponding to various temperatures. When the temperature decreases steadily, the shear adhesion strength increases initially. Then, when the temperature decreases to about −15°C, the adhesion strength reaches its maximum value of about 0.28 MPa. Thereafter, as the temperature continues to decrease further, the shear adhesion strength begins to decrease in magnitude.

Figure 7 illustrates that the experimental data could be fitted nicely into a spline curve. The formula of the curve is as follows:

$$A_d = 0.21016 + 0.06318x + 0.0098x^2 + 3.9712\times10^{-5}x^3 \tag{3}$$

Where, x is the value of temperature (°C).

Table 4 Effects of MVD on experimental results.

MVD/μm	ice thickness/mm	Shear adhesion strength /MPa
22.4	3.12	0.15924
25.5	3.10	0.1672
31.1	2.95	0.2707
38.3	3.02	0.25478
39.8	3.05	0.25032

Figure 8 shows the difference between the experimental data and the calculated results that were obtained using formula (3). The residual results are less than 5% in all 20 test specimens. Therefore, it can be inferred that the formula (3) appropriately describes the relationship between shear adhesion strength and temperature.

3.2 Effects of MVD

In the icing wind tunnel, set the freezing temperature to −8°C. The loading rate is maintained constant at 0.00375 cm/s. The specimen of an aluminum cylinder is used in this experiment; the surface roughness of the aforementioned specimen is 3.19 μm. The freezing time is 4 minutes. Then the values of MVD are changed steadily, and the corresponding values of shear adhesion strength are measured. The experimental data thus obtained is presented in Table 4.

As shown in Table 4, the MVD parameter is changed from 20 to 40 μm. However, the adhesion strength does not become a monotonic function of MVD values. Under the existing experimental conditions, the shear adhesion strength seems to increase initially, and then decrease slowly. In Table 4, when the value of MVD is 31.1 μm, the shear adhesion attains its maximum value. This is because the physical properties of ice are different in different meteorological conditions. In this experiment, the freezing ice is a typical example of glaze

https://doi.org/10.1017/jmech.2017.83 Published online by Cambridge University Press



Fig. 9 Ice photo on the test model (MVD = 31.1 μm).

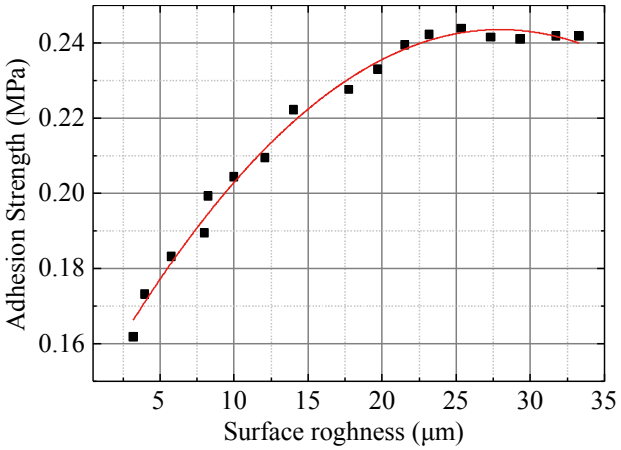


Fig. 10 Shear adhesion strength distribution at different substrate roughness.

ice, as shown in Fig. 9, and the shear adhesion strength is relative large when the value of MVD is 31.1 μm.

3.3 Effects of Substrate Roughness

Seventeen groups of aluminum rod with different surface roughness were included in this experiment. The test parameters are as follows: MVD is 22 μm; the temperature is -8°C, the loading rate is 0.00375 cm/s, and the freezing time is 4min. Fig. 10 shows the different experimental results obtained using aluminum rods with different surface roughness.

As shown in Fig. 10, the implications of the experimental data are as follows: when the same substrate material is used and only the surface roughness is changed continuously from 3 to 33μm, the adhesion strength increases with an increase in surface roughness. From the experimental data curve, it can be inferred that an approximately quadratic relationship exists between the adhesion strength and surface roughness. As shown in Fig. 10, the relation between the shear adhesion strength and the roughness of the substrate is as follows:

$$A_d = 0.14504 + 0.00705x - 1.262\times10^{-4}x^2 \qquad (4)$$

Where, x is the value of roughness (μm).

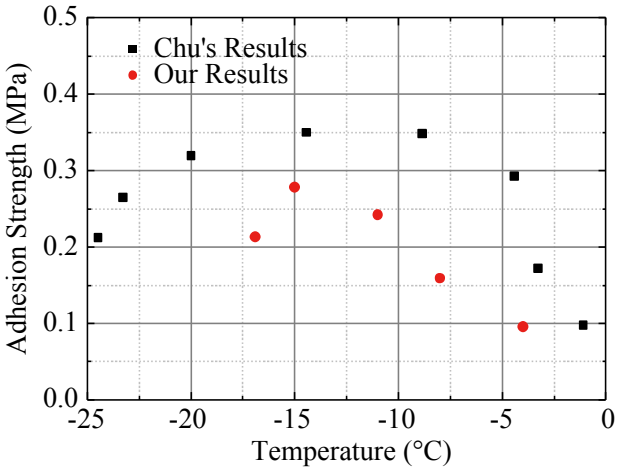


Fig. 11 Compared results of shear adhesion strength versus temperature.

3.4 Comparison with Research Results and Error Analysis

According to the experimental data in this study, the shear adhesion strength of ice lies in the range of 0.084 to 0.28 MPa under the following conditions: the freezing temperature is varied from –4 to –18°C, while MVD values are also varied from 20 to 40 μm, and the substrate material surface roughness is varied from 3 to 33 μm. In the experiments performed by R. J. Scavuzzo and M. L. Chu, with continuously changing the freezing temperature, the surface roughness of the test sample, they found that the shear adhesion strength of impact ice is between 0.09 and 0.35 MPa. We compared the experimental data of Chu *et al* with the experimental results of our study. As shown in Fig. 11 [4], the shear adhesion strength is plotted against various temperatures by referring to the two sets of experimental results.

The experimental data of this study is agrees with that obtained by Chu *et al*. The comparison shows that the two experimental data sets agree in terms of magnitude and trends of change. It is important to note that the measurements of Chu illustrate that the shear adhesion strength reaches its peak at –12°C, whereas the peak appeared at a temperature of nearly -15°C in this study. Moreover, there are errors of shear adhesion strength at other temperatures. This is mainly because of the following reasons: (1) the test conditions are not exactly equal (Chu's experiment conditions: MVD is 20 μm, LWC is 1.3 g/m^3, and the roughness is not specified. Our experiment conditions: MVD is 22 μm, LWC is 1.0 g/m^3, and the roughness is 3.19 μm); and (2) there are differences between the two kinds of measurement methods. Chu's experiments of icing are conducted in the tunnel, and then the test samples are moved out of the tunnel to another low-temperature environment for the purpose of measuring shear force. Thus, differences in the ambient temperature and freezing temperature occur as the test samples are moved from one environment to another. Consequently, the surface of the sample witnesses melting of ice, but it freezes again when it is placed in another cold environment. All these changes

https://doi.org/10.1017/jmech.2017.83 Published online by Cambridge University Press

cause the errors in the measurement of shear adhesion strength between the ice layer and the surface. This drawback of the process followed by Chu *et al* is overcome by an innovative approach in our experiment: the icing test is conducted in an ice tunnel that simulates the flow field of cold air at a high altitude, and the measurements of shear force are obtained in the same temperature environment of the tunnel. Thus, the errors caused by environmental changes are eliminated, and the experimental values are closer to the real values.

4. CONCLUSIONS

Using an icing wind tunnel, the test platform was developed for this study. With this experimental assembly, icing test and measurements of shear adhesion strength were conducted in the interface of ice layers and substrates. The proposed experimental method is designed and performed with precision using the following precautions: the loading speed of force is controlled precisely using stepper motors, whereas pressure transducers measure the shear strength of test samples.

In this experiment, researchers investigated the effects of various meteorological parameters, such as temperature, MVD, and substance roughness. The experimental results indicate that three parameters do have significant effects on the shear adhesion strength. For example, the effects of temperature were quite significant on shear adhesion strength when the surface roughness of the aluminum cylinder was 2.0 μm and the MVD value was 22 μm. The shear adhesion strength between the ice layers and its substrates increases initially with the decrease of temperature, and the maximum shear adhesion strength appears at about –15°C. Then, the shear adhesion strength reduces with a further decline in temperature. To design a novel model of mechanical de-icing system, the experimental results of this study can be used as an excellent reference for understanding shear stress at different temperatures.

ACKNOWLEDGEMENTS

This work was funded by the National Nature Science Foundation [grant number 11402114] and the National Basic Research Program of China (973 Program) [grant number 2015CB755800].

REFERENCES

1. Li, Q.-Y., Zhu, C.-L. and Bai, T., "De-Icing Experiment and Numerical Simulation of the Electro-Impulse De-Icing System," *Journal of Aerospace Power*, DOI:10.13224/j.cnki.jasp.2012.02.020 (2013).
2. Palacios, J.-L., Zhu, Y. and Smith, E.-C., "Ultrasonic Shear and Lamb Wave Interface Stress for Helicopter Rotor De-Icing Purposes," *Proceedings of 47th AIAA/ASME/ASCE/AHS/ASC Structures, Structural Dynamics, and Materials Conference*, Rhode Island, America (2006).
3. Zhu, Y., Palacios, J.-L., Rose, J.-L. and Smith, E.-C., "Numerical Simulation and Experimental Validation of Tailored Wave Guides for Ultrasonic De-Icing on Aluminum Plates," *Proceedings of 51th AIAA/ASME/ASCE/AHS/ASC Structures, Structural Dynamics, and Materials Conference*, Florida, America (2010).
4. Guy, F. and Jean, P., "Ice Adhesion Models to Predict Shear Stress at Shedding," *Journal of Adhesion Science and Technology*, **26**, pp. 523-553 (2012).
5. Petrenko, V. F. and Peng, S., "Reduction of Ice Adhesion to Mental by Using Self-Assembling Monolayers," *Canadian Journal of Physics*, **81**, pp. 387-393 (2003).
6. Scavuzzo, R.-J. and Chu, M.-L., "Structural Properties of Impact Ices Accreted on Aircraft Structures," NAS 1.26179580: NASA-CR-179580, 87N18121 (1987).
7. Druez, J., Phan, C.-L. and Laforte, J.-L., "The Adhesion of Glaze and Rime on Aluminum Electric Conductors," *Transactions CSME*, **5**, pp. 215-220 (1979).
8. Jellinek, H.-G., "The Influence of Imperfections on the Strength of Ice," *Journal of Applied Physics*, **27**, pp. 1198-1209 (1958).
9. Stallbrass, J.-R. and Price, R.-D., "Study on the Adhesion of Ice to Various Materials," *National Research Council*, NRC No. 6980 (1963).
10. Meuler, A.-J., Smith, J.-D., Varanasi, K.-K., Mabry, J.-M. and Mckinley, G.-H., "Relationships Between Water Wettability and Ice Adhesion," *Acs Applied Materials & Interfaces*, **2**, pp. 3100-3110 (2010).
11. Miller, T.-L. and Bond, T. H., "Icing Research Tunnel Test of a Model Helicopter Rotor," NASA TM-101978 (1989).
12. Reich, A.-D., "Comparison of Rime and Glaze Deformation and Failure Properties," *AIAA*, **91**, 0446 (1991).
13. Li, H.-S. and Du, X.-Z., "The Constitutive Theory of Damage and Fracture of Ice Materials Frozen Soil," *Journal of Glaciology and Geocryology*, **25**, pp. 304-307 (2003).
14. Yue, Q.-J., Zhou, X.-A. and Shen, W., "The Experimental Method of Shear Strength of Glaze Ice," *Journal of Glaciology and Geocryology*, **16**, pp. 75-79 (1994).
15. Liu, W.-B., Li, G.-W. and Wang, L.-Y., "Study on Shear Strength and Modulus of Fresh Water Ice by Torsion Test," *Journal of Dalian University of Technology*, **39**, pp. 31-33 (1999).
16. Anderson, D. *et al*., "Tests of the Performance of Coatings for Low Ice Adhesion," *A9715374, AIAA*, **97**, 0303 (1997).
17. Ivan, A.-R. and Petrenko, V.-F., "Physical Mechanisms Responsible for Ice Adhesion," *Journal of*

https://doi.org/10.1017/jmech.2017.83 Published online by Cambridge University Press

Physical Chemistry B, **101**, pp. 6267-6270 (1997).

18. Yin, L., Xia, Q. and Xue, J., "In Situ Investigation of Ice Formation on Surfaces with Representative Wettability," *Applied Surface Science*, **256**, pp. 6764-6769 (2010).
19. Wang, F., Lv, F. and Liu, Y.-P., "Ice Adhesion on Different Microstructure Super Hydrophobic Aluminum Surface," *Journal of Adhesion Science and Thechology*, **27**, pp. 58-67 (2013).
20. Haneesh, K., Joseph, C. and Pruitt, B.-L., "Role of Surface Roughness in Hysteresis during Adhesive Elastic Contact. Philosophical Magazine Letters," **90**, pp. 891-902 (2010).

(Manuscript received January 19, 2017,
accepted for publication July 24, 2017.)

https://doi.org/10.1017/jmech.2017.83 Published online by Cambridge University Press